Archives of Mechanics • Archiwum Mechaniki Stosowanej • 28, 5-6, pp. 1011–1024, Warszawa 1976

On the motion of a rotating fluid in the presence of an infinite rotating disk

P. D. WEIDMAN AND L. G. REDEKOPP (LOS ANGELES)

THE MODIFIED Kármán equations describing the fluid motion above a rotating disk are investigated by means of a regular perturbation expansion in terms of the Rossby number $\varepsilon = \Omega/\omega$, where ω is the angular velocity of the fluid and Ω is the angular velocity of the plate. Analysis of the coefficients of the series expressions for the plate friction and the Ekman flux, together with complete numerical solutions, reveals that there is a singularity near $\varepsilon = \varepsilon_0 = -0.154$. The singularity appears to have physical significance in that the meridianal streamline flow is of onecell type for $\varepsilon > \varepsilon_0$ and of two-cell type for $\varepsilon < \varepsilon_0$. We propose that the bifurcation of the flow for $\varepsilon \gtrless \varepsilon_0$ is responsible for the failure to obtain numerical solutions for a range of negative Rossby numbers.

Zmodyfikowane równania Kármána, opisujące ruch wirującej tarczy, zostały zbadane za pomocą regularnego rozwinięcia perturbacyjnego, przyjmując jako mały parametr liczbę Rossby'ego $\varepsilon = \varepsilon/\Omega$, gdzie ω oznacza prędkość kątową cieczy, a Ω jest prędkością kątową płyty. Analiza współczynników szeregów wyrażających tarcie płyty i strumień Ekmana wraz z kompletnymi rozwiązaniami numerycznymi wykazują, że w otoczeniu $\varepsilon = \varepsilon_0 = -0.154$ występuje osobliwość. Jak się okazuje osobliwość ta posiada określony sens fizykalny. Mianowicie oznacza, że przepływ linii prądu w kierunku południowym jest typu jednokomórkowego dla $\varepsilon > \varepsilon_0$ i typu dwukomórkowego dla $\varepsilon < \varepsilon_0$. Stąd nasuwa się wniosek, że bifurkacja przepływu dla $\varepsilon \gtrless \varepsilon_0$ jest odpowiedzialna za niemożność otrzymania rozwiązania numerycznego dla zakresu ujemnych liczb Rossby'ego.

Модифицированные уравнения Кармана, описывающие движение вращающегося диска, исследованы при помощи регулярного пертурбационного разложения, принимая как малый параметр ε число Россби $\varepsilon = \omega/\Omega$, где ω обозначает угловую скорость жидкости, Ω является угловой скоростью плиты. Анализ коэффициентов рядов, выражающих трение плиты и поток Экмана, совместно с полными численными решениями, показывает, что в окрестности $\varepsilon = \varepsilon_0 = -0{,}154$ выступает особенность. Как оказывается эта особенность имеет определенный физический смысл. Именно она обозначает, что течение линии тока в меридиональном направлении является одноячейкового типа для $\varepsilon > \varepsilon_0$ и двуячейкового типа для $\varepsilon < \varepsilon_0$. Оттуда следует вывод, что бифуркация течения для $\varepsilon \lessgtr \varepsilon_0$ ответственна за невозможность получения численного решения для области отрицательных чисел Россби.

1. Introduction

THE FLUID motion created by an infinite disk rotating at a rate different from the ambient fluid has stimulated considerable interest since it was first discussed by VON KÁRMÁN (1921). The problem was subsequently considered by COCHRAN (1934) and BÖDEWADT (1940), but, perhaps, the most definitive results were presented by ROGERS and LANCE (1960), hereafter referred to as *R* and *L*. The latter investigators presented accurate numerical solutions covering the entire range of positive Rossby number $\varepsilon = \omega/\Omega$, where ω is the rotational speed of the fluid bounded below by a disk rotating at angular velocity Ω. Kármán studied the problem in which the plate rotates beneath a quiescent fluid ($\varepsilon = 0$)

and Bödewadt studied the configuration in which the fluid rotates above a stationary plate ($\varepsilon = \infty$). The classical linearized Ekman boundary layer flow corresponds to ε near unity. For negative values of ε, when the fluid and plate rotate in opposite directions, R and L have reported numerical solutions for $\varepsilon = -0.05$, -0.10, and -0.15; for more negative values of ε, however, the solutions did not converge sensibly and even the reported solutions appeared unacceptable on physical grounds — the plate friction, for example, was observed to decrease with an increase in the relative velocity between plate and fluid.

In this study we obtain expressions for the plate friction and Ekman suction as a function of the Rossby number by means of a regular expansion of the modified von Kármán equations in powers of ε and integrating the resulting system of equations. The preliminary motivation was to verify the anomalous behavior of the Ekman pumping found by R and L for small positive Rossby number. The non-monotonic dependence of the Ekman suction on ε leads to some interesting results when used in conjunction with the Wedemeyer model for non-linear spin-up of a contained fluid (WEIDMAN, 1973). An analysis of our perturbation solutions, however, brings forth a more interesting fact: the Kármán similarity equations exhibit a singularity near $\varepsilon \cong -0.154$. We believe that this singular behavior in some way must account for the problems of convergence encountered by R and L beyond $\varepsilon = -0.15$.

2. Equations and solutions

The Navier-Stokes equations for the rotationally symmetric flow of an incompressible, viscous fluid can be reduced to the form (cf. SCHLICHTING (1962))

$$\begin{aligned} F'' &= F^2 - G^2 + HF' + \varepsilon^2, \\ G'' &= 2FG + HG', \\ H' &= -2F, \end{aligned} \tag{2.1}$$

where the prime denotes differentiation with respect to the similarity variable $\zeta = z\sqrt{\frac{\Omega}{\nu}}$ and ε is the Rossby number defined previously. The radial, azimuthal and vertical velocity components are given by

$$\begin{aligned} u(r, \zeta) &= r\Omega F(\zeta), \\ v(r, \zeta) &= r\Omega G(\zeta), \\ w(r, \zeta) &= \sqrt{\nu\Omega} H(\zeta). \end{aligned} \tag{2.2}$$

We note that the equations are an exact reduction of the Navier-Stokes equations when we consider a semi-infinite fluid rotating above a disk of infinite radial extent. The boundary conditions for this case are

$$\begin{aligned} F(0) = H(0) = 0, \quad G(0) = 1, \\ F(\infty) = 0, \quad G(\infty) = \varepsilon. \end{aligned} \tag{2.3}$$

We seek a solution which can be expanded as a regular perturbation series in ε

$$\begin{Bmatrix} F(\zeta) \\ G(\zeta) \\ H(\zeta) \end{Bmatrix} = \sum_{n=0}^{\infty} \varepsilon^n \begin{Bmatrix} F_n(\zeta) \\ G_n(\zeta) \\ H_n(\zeta) \end{Bmatrix}, \tag{2.4}$$

noting that the basic motion ($\varepsilon = 0$) is the Kármán flow. Insering (2.4) into (2.1), one obtains the ordered set of equations

$$\begin{aligned} F_n''' &= \sum_{j=0}^{n} (F_j F_{n-j} - G_j G_{n-j} + H_j F_{n-j}) + \delta_{2n}, \\ G_n'' &= \sum_{j=0}^{n} (F_j G_{n-j} + H_j G_{n-j}'), \\ H_n' &= -2F_n, \end{aligned} \tag{2.5}$$

where δ_{mn} is the Kronecker delta. The boundary conditions (2.3) can now be written

$$\begin{aligned} F_n(0) &= H_n(0) = 0, \quad G_n(0) = \delta_{0n}, \\ F_n(\infty) &= 0, \quad G_n(\infty) = \delta_{1n}. \end{aligned} \tag{2.6}$$

The procedure for solving the above system of equations is to successively integrate each set of equations (2.5) and satisfy the boundary conditions for each order (2.6) by iterations on $F_n'(0)$ and $G_n'(0)$. The zeroeth order Kármán equations are non-linear, but the higher order equations are linear and, in principle, pose no problem of convergence for a high speed computer. The question of selecting "infinity", however, does cause practical limitations. In order to elucidate this difficulty we briefly examine the asymptotic behavior of the perturbation solutions for large ζ.

Consider the following form of the solutions assumed valid in the limit $\zeta \to \infty$:

$$\begin{aligned} F(\zeta) &\sim \sum_{n=0}^{\infty} f_n(\zeta)\varepsilon^n, \\ G(\zeta) &\sim \sum_{n=0}^{\infty} (g_n(\zeta) + \delta_{2n})\varepsilon^n, \\ H(\zeta) &\sim \sum_{n=0}^{\infty} (H_n(\infty) + h_n(\zeta))\varepsilon^n. \end{aligned} \tag{2.7}$$

Here $H_n(\infty)$ is the Ekman suction and each nth order solution satisfies the boundary conditions $(2.6)_2$ provided

$$\lim_{\zeta \to \infty} \begin{Bmatrix} f_n(\zeta) \\ g_n(\zeta) \\ h_n(\zeta) \end{Bmatrix} = \begin{Bmatrix} 0 \\ 0 \\ 0 \end{Bmatrix}. \tag{2.8}$$

Inserting the expressions (2.7) into the equations of motion (2.1), one obtains a set of linear equations the solutions of which have the behavior

$$\begin{Bmatrix} f_n(\zeta) \\ g_n(\zeta) \\ h_n(\zeta) \end{Bmatrix} \sim \begin{Bmatrix} a_n \\ b_n \\ c_n \end{Bmatrix} \zeta^n \exp(H_0(\infty)\zeta), \tag{2.9}$$

where $H_0(\infty) = -0.88446$ is known from the integrations performed by R and L. It is readily apparent that, although the solutions die out exponentially for large ζ, the algebraic modulation pushes "infinity" farther away for each higher order set of equations. In addition, the magnitudes of the coefficients are unknown and could well be large. Suppose for purpose of discussion that the coefficients are 0(1) and we are satisfied to carry our integrations to a distance ζ_∞ for which an error of 10^{-10} or less is incurred. Eq. (2.9) then shows that for $n = 0$, $\zeta_\infty \simeq 25$; $n = 5$, $\zeta_\infty \simeq 50$; and $n = 10$, $\zeta_\infty \simeq 75$. We are cautioned, therefore, not to expect a large number of terms of comparable accuracy in the perturbation solutions.

The equations of motion (2.5) satisfying the appropriate boundary conditions (2.6) were successively integrated in double precision to order $n = 8$ on a PDP-10 digital computer. Hammings modified predictor-corrector integration scheme with variable step size was employed. Rounded-off errors were kept less than 10^{-14} for all numerical computations to be presented. The Taylor expansion interpolation scheme used by R and L was also incorporated here to iterate in the sequel. Initially the nine sets of equations were integrated

Table 1

n	$F_n'(0)$	$G_n'(0)$	$H_n(\infty)$
0	0.5102326188673	−0.6159220143993	−0.88447411021
1	0.109311401	0.0516237127	−1.13035202
2	−0.79579343	1.04439386	11.005861
3	0.1591134	−1.5779433	−41.045331
4	0.498574	4.62448	150.851
5	−2.7291	−17.2071	−595.32
6	11.977	73.35	2534.
7	−53.0	−340.0	-1.15×10^4
8	244.	1.66×10^4	5.5×10^4

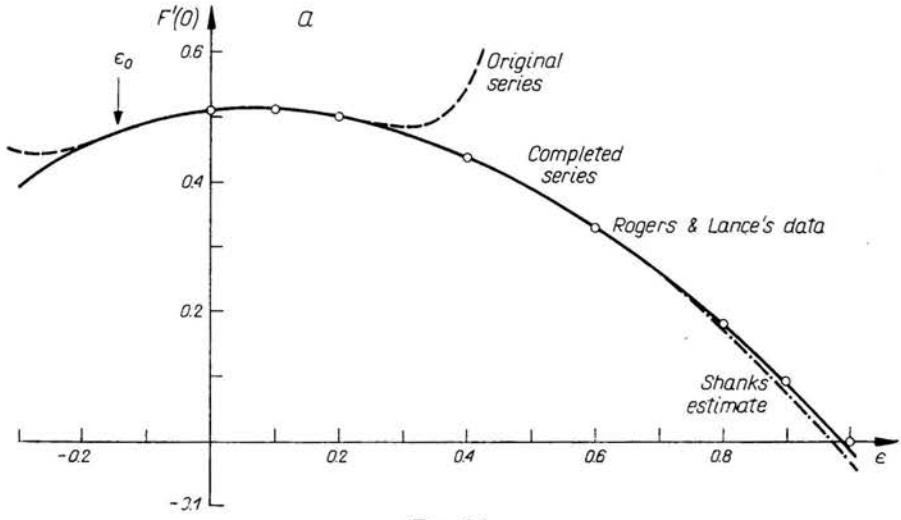

(FIG. 1.)

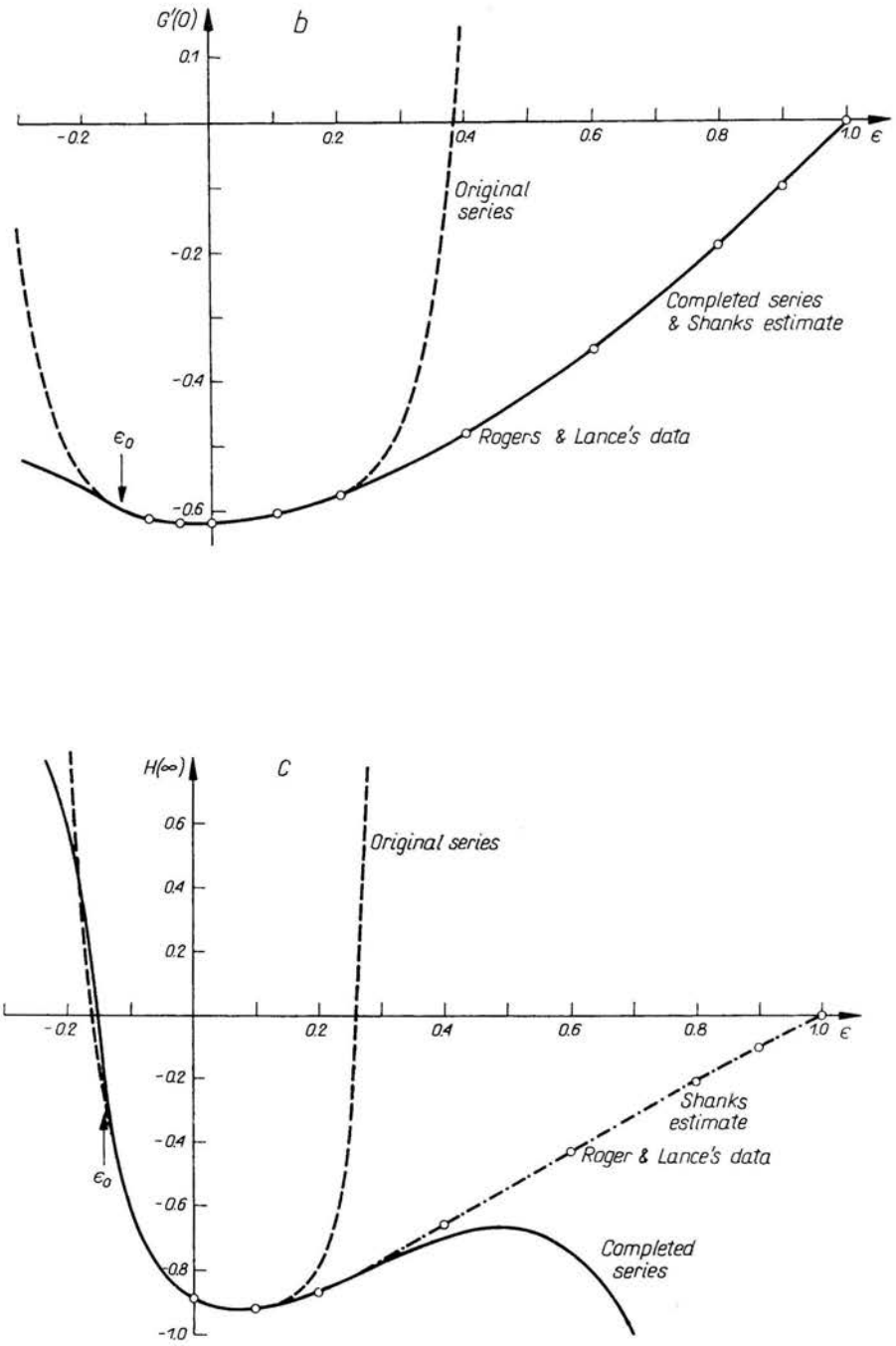

FIG. 1. a) Radial friction $F'(0)$ as a function of Rossby numbers – – – regular perturbation series; ——— completed series; –·–·– Shanks estimate; ○ Rogers and Lance's computed points; b) same as (a) but for azimuthal friction $G'(0)$; c) same as (a) but for Ekman suction $H(\infty)$.

to $\zeta = 35$, and subsequently each set was again integrated to $\zeta = 70$. In Table 1 we present the coefficients for the plate friction $F_n'(0)$, $G_n'(0)$, as well as those for the Ekman suction $H_n(\infty)$. Only the significant figures for which the results at $\zeta = 70$ agree with those at $\zeta = 35$ are listed. Even the repeatability of the significant figures at the two integration lengths does not insure their correctness. We, in fact, use the results of R and L to help ascertain the accuracy of our own computations. In Figs. 1(a), (b) and (c) we have plotted as a dashed line the computations for $F'(0)$, $G'(0)$, and $H(\infty)$ as a function of the Rossby number; the open dots are the calculated points due to R and L. Agreement is obtained only in the range $|\varepsilon| < 0.15$, approximately, and the expansions diverge rapidly for large positive ε. Although it appears that our perturbation series has a relatively small radius of convergence, it seems large enough to substantiate the nonmonotonic behavior of $F'(0)$ and $H(\infty)$ for small positive Rossby numbers. Moreover, the decrease in azimuthal friction $G'(0)$ for small negative ε reported by R and L is also verified.

3. Improvement of the perturbation expansions

In order to make full use of the numerical results thus obtained, one can incorporate various techniques to determine and sometimes improve the radius of convergence of a perturbation series. At the same time, information can be obtained about the nature of the nearest singularity. The methods used in this section are summarized in a recent paper by VAN DYKE (1974).

In the series expansion $\sum_n C_n \varepsilon^n$, a plot of the ratios of succeeding coefficients C_n/C_{n-1} versus $1/n$, known as the Domb Sykes plot, will generally reveal a regular pattern after a sufficient number of terms. This diagram is particularly useful for determining the location and nature of the nearest singularity for a given series, especially if the singular behavior is simple as in the model function

$$f(\varepsilon) = \text{const}\,(\varepsilon \pm \varepsilon_0)^{\alpha}, \tag{3.1}$$

where α is not a non-negative integer. In this case, the inverse ratio of coefficients will plot linearly with $1/n$, such that

$$\frac{C_n}{C_{n-1}} = \mp \frac{1}{\varepsilon_0}\left[1 - \frac{1+\alpha}{n}\right]. \tag{3.2}$$

A Domb Sykes diagram of the coefficients for $F'(0)$, $G'(0)$, and $H(\infty)$, given in Figs. 2(a), (b) and (c), suggests the existence of just such a simple singularity, particularly the plot for $G'(0)$. A linear least squares fit to the last six points gives $\alpha = 1.34$ and, following the suggestion of VAN DYKE (1974), we pick the nearest integer or simple fraction. The value of ε_0 is determined by selecting $\alpha = 4/3$ and least squares fitting the four interior points on the straight line in Fig. 2 (b); the first of the six points is neglected since it may not yet have settled into a regular pattern, and the last point is omitted because its accuracy is suspect. The singular point is found to have a magnitude $\varepsilon_0 = 0.1433$ (very close to 1/7) and lies on the negative real axis. The straight line corresponding to $\alpha = 4/3$ and $\varepsilon_0 = 0.1433$ is sketched as a dashed line in Figs. 2 (a) and (c). It seems plausible that both $F'(0)$ and $H(\infty)$ also exhibit the same singular behavior as $G'(0)$.

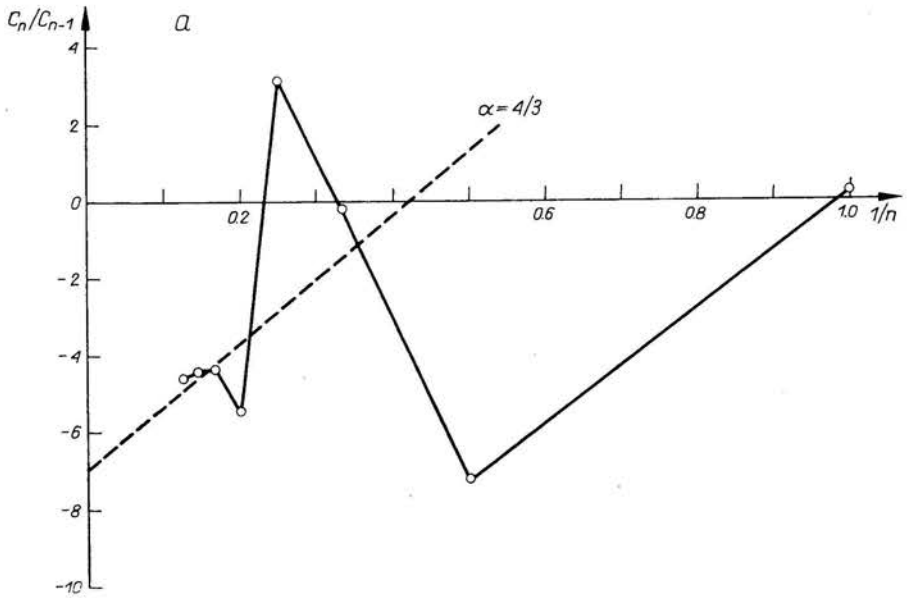

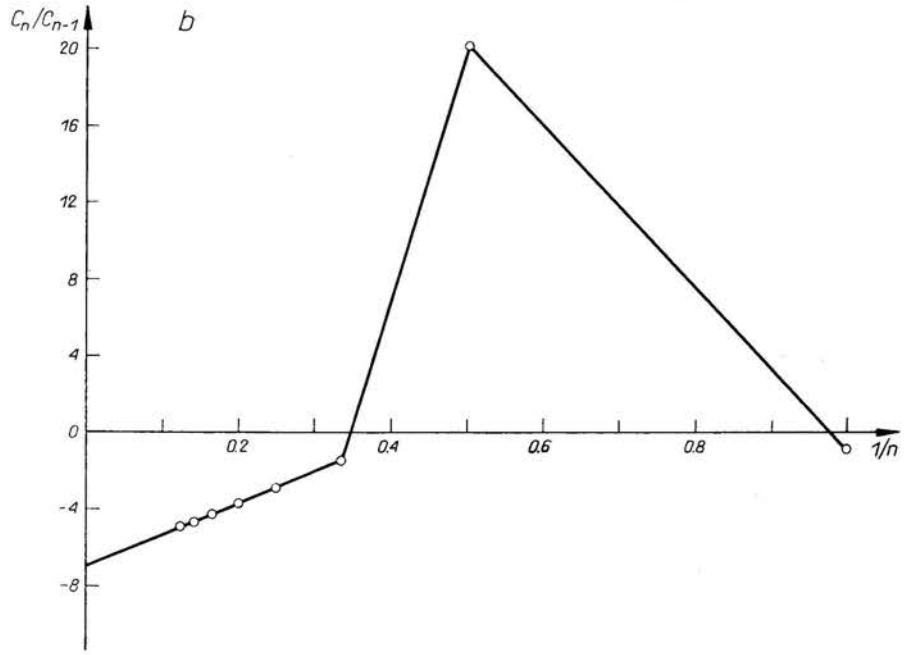

(FIG. 2.)

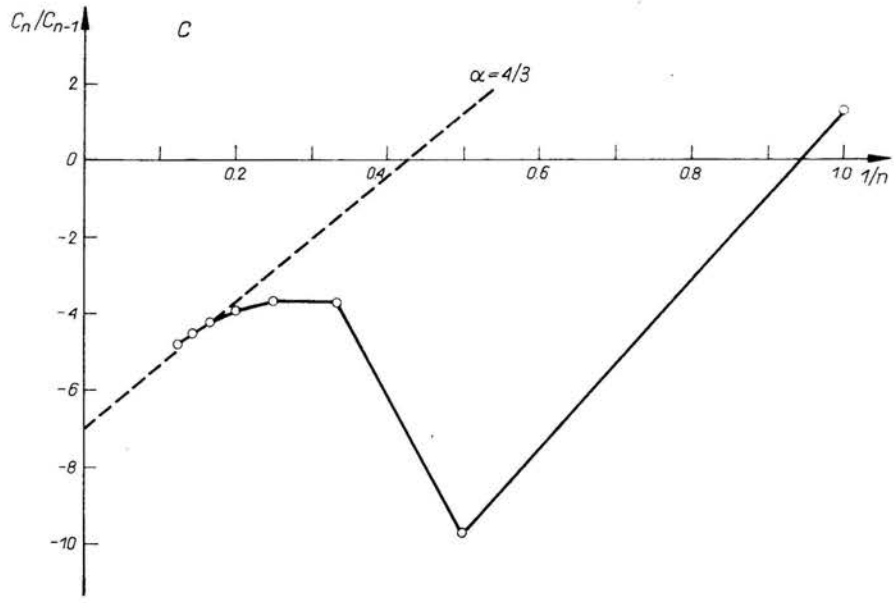

FIG. 2. Domb Sykes plot of regular perturbation series for: a) the radial friction $F'(0)$, b) the azimutha friction $G'(0)$, and (c) the Ekman suction $H(\infty)$.

Knowing the nature and location of the primary singularity, one can attempt to improve the series by extracting the leading singularity multiplicatively, which, for our model function (3.1), leads to the form

$$f(\varepsilon) = (\varepsilon+\varepsilon_0)^{\alpha} \sum_n a_n \varepsilon^n. \tag{3.3}$$

This was done for $F'(0)$ and $G'(0)$, and $H(\infty)$ and the Domb Sykes plot of the ratios a_n/a_{n-1} are given in Figs. 3 (a), (b) and (c). The secondary singularity for $F'(0)$ and $G'(0)$ lies at the same location as the primary one and is of order $\alpha = -4/3$ for the multiplicative series in the representation given by (3.3). The Domb Sykes plot for the secondary series of $H(\infty)$ has not yet settled down, but it evidently will not approach ε_0 in the same manner as the frictional coefficients.

Since the secondary singularities for $F'(0)$, $G'(0)$, and most probably $H(\infty)$ lie at the same location as the primary singularity, the latter must be extracted additively rather than multiplicatively. However, since the strength of the primary singularity is not known, an additive extraction is not possible.

Another method for extending the range of applicability of each series is to map the singularity to infinity using, for example, the Euler transformation $\delta = \varepsilon/(\varepsilon+\varepsilon_0)$ and rewriting the series as $\sum_n b_n \delta^n$. The Domb Sykes diagram of the resulting coefficient ratios b_n/b_{n-1} for $F'(0)$, $G'(0)$, and $H(\infty)$ are presented in Figs. 4 (a), (b) and (c). The plots for $F'(0)$ and $G'(0)$ are seen to asymptote to $\delta_0 = 1$ with $\alpha = -1$; it is possible that the plot for $H(\infty)$ will also oscillate about this asymptote. One concludes, therefore,

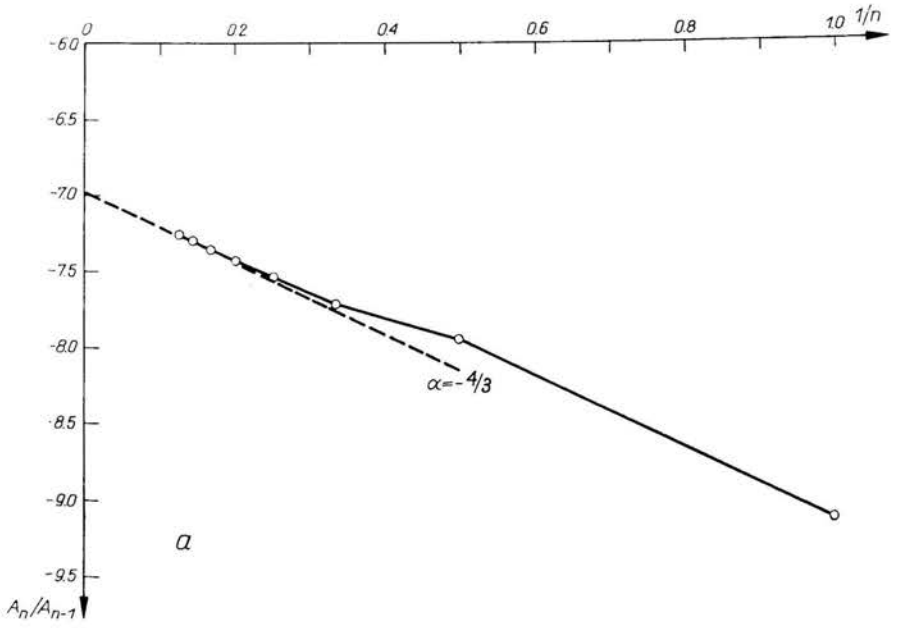

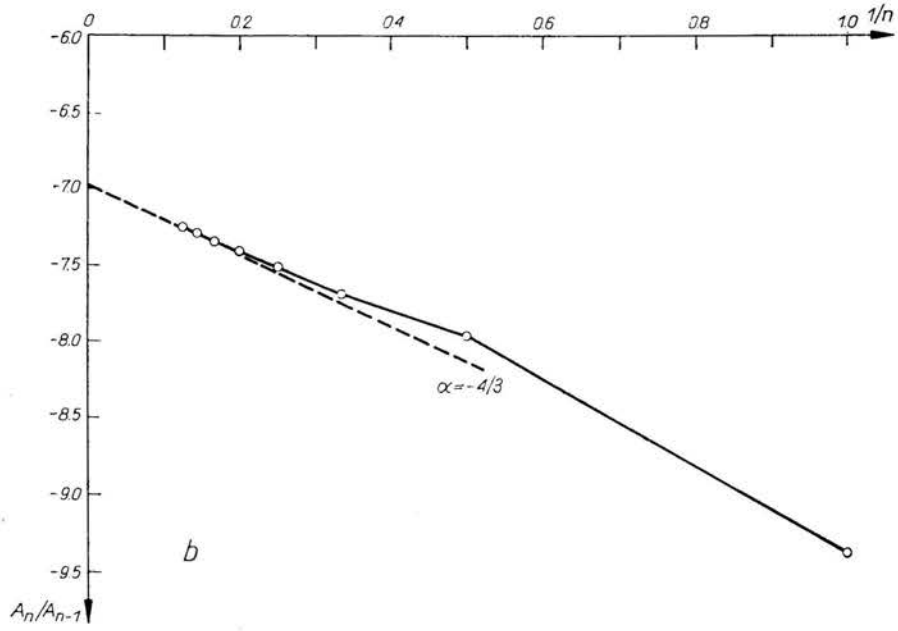

(FIG. 3.)

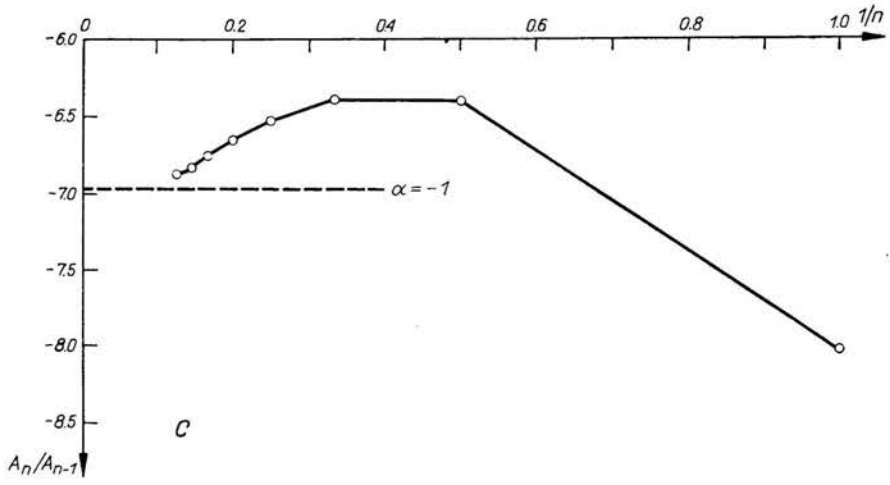

FIG. 3. Domb Sykes plot of secondary series from a multiplicative extraction of $(\varepsilon+0.1433)^{4/3}$ for: a) radial friction $F'(0)$, b) the azimuthal friction $G'(0)$, and c) the Ekman suction $H(\infty)$.

that the Euler expansions are singular at $\delta = \infty$ and the calculations (not plotted) for $F'(0)$, $G'(0)$, and $H(\infty)$ show little improvement over the original perturbation expansions for positive Rossby numbers. However, the Domb Sykes plots for the Euler series are useful because, if the coefficients do converge to $\delta_0 = 1$ as we infer, then not only is ε_0 the nearest singularity, but it is the only singular point except, perhaps, at $\varepsilon = \pm\infty$.

When sufficient confidence in the values of ε_0 and α of the primary singularity is obtained, improved convergence can often be had by completing the series. In this procedure the remainder after N terms of the original series is taken to be proportional to the remain-

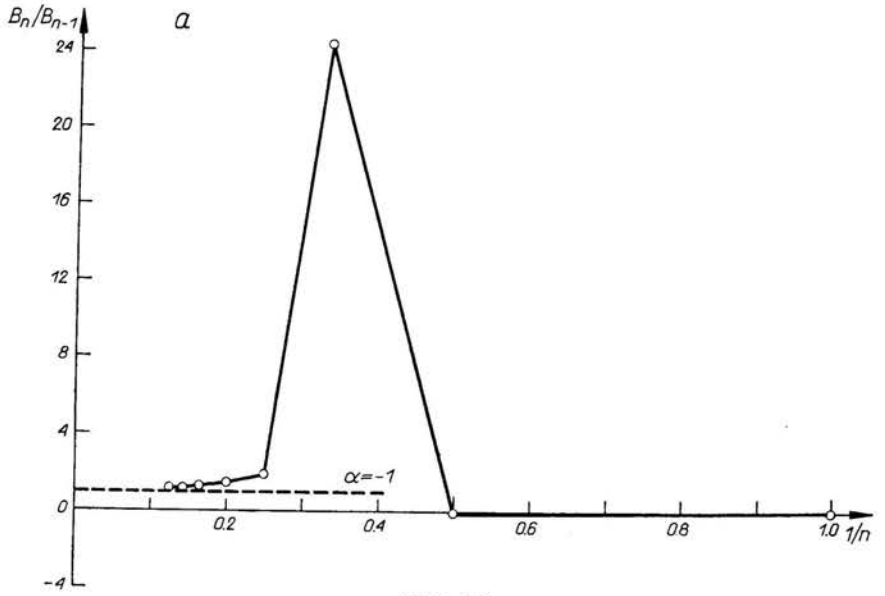

(FIG. 4.)

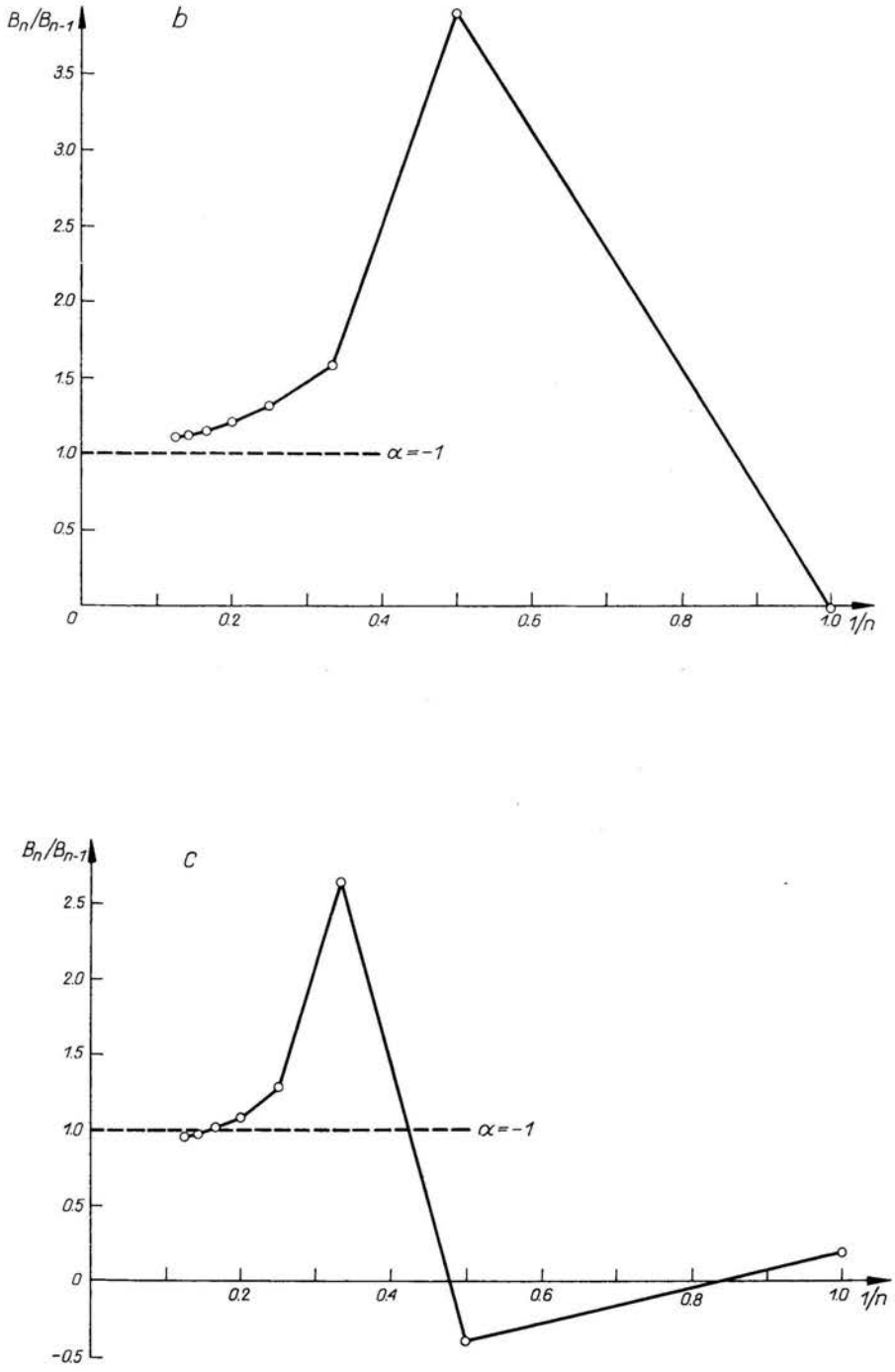

FIG. 4. Domb Sykes plot of the series resulting from the Euler transformation $\varepsilon/(\varepsilon+\varepsilon_0)$ for: a) the radial friction $F'(0)$, b) the azimuthal friction $G'(0)$, and (c) the Ekman suction $H(\infty)$.

der in the binomial expansion of $(\varepsilon \pm \varepsilon_0)^\alpha$, and this is effected by matching the coefficients of ε^N in each expansion. The completed series for the model function (3.1) is given by

$$(3.4)\quad f(\varepsilon) \cong \sum_{n=0}^{N-1} C_n \varepsilon^n + (\mp \varepsilon_0)^N \frac{N!(-1-\alpha)!}{(N-1-\alpha)!} C_n \left[\left(1 \pm \frac{\varepsilon}{\varepsilon_0}\right)^\alpha - \sum_{n=0}^{N-1} \frac{(n-1-\alpha)!}{n!(-1-\alpha)!} \left(\mp \frac{\varepsilon}{\varepsilon_0}\right)^n \right].$$

The completed series for $F'(0)$, $G'(0)$, and $H(\infty)$ given below were obtained by matching coefficients at $N = 6$, since higher order matchings proved less accurate when compared with the data of R and L

$$\begin{aligned} F'(0) &\cong 0.206226(\varepsilon+\varepsilon_0)^{4/3} + 0.494768 - 0.034579\varepsilon \\ &\quad - 0.96315\varepsilon^2 + 0.4186\varepsilon^3 - 0.256\varepsilon^4 + 0.079\varepsilon^5, \\ G'(0) &\cong 1.263029(\varepsilon+\varepsilon_0)^{4/3} - 0.710635 - 0.829630\varepsilon \\ &\quad + 0.01944\varepsilon^2 + 0.0115\varepsilon^3 + 0.003\varepsilon^4 - 0.007\varepsilon^5, \\ H(\infty) &\cong 43.63641(\varepsilon+\varepsilon_0)^{4/3} - 4.156705 + 31.57679\varepsilon \\ &\quad - 24.4052\varepsilon^2 + 13.868\varepsilon^3 - 8.819\varepsilon^4 - 1.060\varepsilon^5. \end{aligned} \tag{3.5}$$

The values computed from the above equations are presented in Figs. 1 (a), (b), and (c) for comparison with the original perturbation expansions. The range of convergence for both $F'(0)$ and $G'(0)$ is significantly extended; graphical comparison with R and L's computed points indicate an improved range of utility to $\varepsilon \cong 0.8$ for $F'(0)$ and to $\varepsilon > 1.0$ for $G'(0)$. The range of convergence for $H(\infty)$, however, is only approximately double what of the original series for positive ε. Success with Eq. (3.4) for series completion evidently depends strongly on the accuracy of the Nth coefficient of the series. The Domb Sykes plots in Figs. 3 and 4 suggest that the $H(\infty)$ coefficients are less accurate than those for the plate friction $F'(0)$ and $G'(0)$, and hence the relatively small extended range of convergence for the completed series of the Ekman suction could be anticipated.

In a final attempt to improve the convergence of our results, we have applied Shanks' transformation to our series. The Shanks method, exact for geometrical sequences, estimates the limiting value for $n \to \infty$ from any three successive partial sums S_n by the nonlinear transformation (cf. SHANKS (1955))

$$(3.6)\quad e(S_n) = \frac{S_{n+1}S_{n-1} - S_n^2}{S_{n+1} + S_{n-1} - 2S_n}.$$

The results of successive transformations from the first nine partial sums for $F'(0)$ are presented in Fig. 1 (a) as the dash-dot-dash curve. We note that the Shanks transformation considerably extends the range of convergence of the original series, but the estimates are not quite as accurate as the completed series given by $(3.5)_1$. Results from the Shanks transformation applied to $G'(0)$ fall exactly on top of the curve for the completed series in Fig. 1 (b). Actually, the Shanks estimates in this case are considerably more accurate than the completed series given by $(4.5)_2$; the values for $G'(0)$ reproduce R and L's calculations to better than three decimal places in the range $-0.1 \leqslant \varepsilon \leqslant 1.0$. Finally, in Fig. 1 (c) we present the Shanks estimates for $H(\infty)$ computed from the first eight partial sums — the ninth coefficient was sufficiently inaccurate to provide improved results with the Shanks

transformation. The marked improvement in convergence is obvious; all values for $H(\infty)$ obtained in the range $0 \leqslant \varepsilon \leqslant 1.0$ compare to better than two decimal place accuracy with the values reported by R and L.

4. Discussion

Physically, the singular point appears to represent a bifurcation of the flow from a one-cell type, such as exists for $\varepsilon > 0$, to a two-cell type. BATCHELOR (1951) conjectured that for $\varepsilon < 0$ the streamlines in a meridional plane would be divided into two cells by the plane $\zeta = \zeta(H = 0)$. Moreover, he suggested that this dividing plane would move uniformly from $\zeta = 0$ at $\varepsilon = -\infty$ to $\zeta = \infty$ at $\varepsilon = 0$. In Fig. 5 we have sketched the altitude variation of the dividing plane obtained from our numerical results; indeed the plane does fade out to infinity, but it does so before reaching $\varepsilon = 0$. Another means of viewing the problem is to plot the variation of $H(\infty)$ with ε in order to determine when the Ekman flux vanishes. Numerical integration of the full Kármán equations gives, in Fig. 5, a zero intercept at $\varepsilon = -0.154$ and close agreement is obtained from the complete series. We expect that the inclusion of more terms of sufficient accuracy in our expansion will

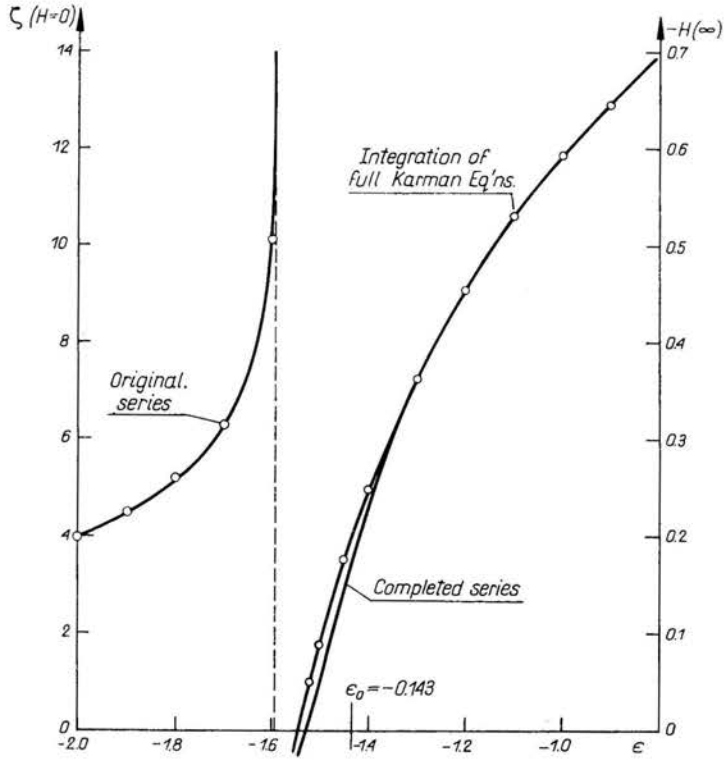

FIG. 5. Variation of the Ekman flux and the level of vanishing normal velocity for negative Rossby numbers.

reveal the trend of $\varepsilon_0 \to -0.154$ in the Domb Sykes plot. We believe that the bifurcation of the motion into a two-cell flow for $\varepsilon < -0.154$ is precisely the reason why many recent attempts to integrate the full equations numerically have failed.

References

1. G. K. BATCHELOR, *Note on a class of solutions of the Navier-Stokes equations representing steady rotationally symmetric flow*, Quart. Mech. Appl. Math., **4**, 29-41, 1951.
2. U. T. BÖDEWAT, *Die Drehstromung über festem Grunde*, Z. angew. Math. Mech., **20**, 241-253, 1940.
3. W. G. COCHRAN, *The flow due to a rotating disc*, Proc. Camb. Phil. Soc., **30**, 365-375, 1934.
4. M. H. ROGERS and G. N. LANCE, *The rotationally symmetric flow of a viscous fluid in the presence of an infinite rotating disk*, J. Fluid Mech., **7**, 617–631, 1960.
5. H. SCHLICHTING, *Boundary layer theory*, Mc Graw-Hill, New York, 84–86, 1960.
6. D. SHANKS, *Non-linear transformation of divergent and slowly convergent sequences*, J. Math. Phys., **34**, 1–42, 1955.
7. P. D. WEIDMAN, *On the spin-up and spin-down of a rotating fluid, Part. 1. Extending the Wedemeyer model*, J. Fluid Mech., **77**, 685—708, 1976.
8. M. VAN DYKE, *Analysis and improvement of perturbation series*, Quart. J. Mech. Appl. Math., 27, 423-450, 1974.
9. T. VON KÁRMÁN, *Über laminare und turbulente Reibung*, Z. angew. Math. Mech., 1, 233–251, 1921.

DEPARTMENT OF AEROSPACE ENGINEERING
UNIVERSITY OF SOUTHERN CALIFORNIA, LOS ANGELES.

Received January 28, 1976.